Theriogenology 236 (2025) 21–32

Contents lists available at ScienceDirect

Theriogenology

journal homepage: www.theriojournal.com

Original Research Article

# The regulatory repertoire of ZBTB16 in porcine immature spermatogonia

Youjie Cui [a], Wei Liu [a], Xueni You [a], Wanying Li [a], Ruiqi Wu [a], Wenxian Zeng [a], Weijun Pang [a], Peng Wang [b,**], Yi Zheng [a,*]

[a] Key Laboratory for Animal Genetics, Breeding and Reproduction of Shaanxi Province, College of Animal Science and Technology, Northwest A&F University, Yangling, Shaanxi, 712100, China

[b] Ningxia Key Laboratory of Cerebrocranial Diseases, College of Traditional Chinese Medicine, Ningxia Medical University, Yinchuan, China

ARTICLE INFO

*Keywords:*
ZBTB16
PLZF
Pig
Spermatogonia
Self-renewal
CUT&Tag

ABSTRACT

Spermatogenesis is a highly productive and intricate process occurring in testes that produces functional haploid sperm capable of fertilization therefore sustaining lifelong male fertility. A cornerstone of spermatogenesis is primitive spermatogonia, including spermatogonial stem cells (SSCs), that are able to self-renew and differentiate. The molecular mechanisms for spermatogonial self-renewal and differentiation in large domestic animals such as pigs, in comparison with their counterparts in mice, are poorly understood. In this study, we explored the expression pattern of ZBTB16 (a key transcription factor also known as PLZF) and its regulatory repertoire in porcine immature spermatogonia. We first co-stained ZBTB16 with spermatogonial/proliferative markers (DBA, SALL4, UCHL1 or Ki67) on testis sections from four ages of boars, demonstrating that ZBTB16$^{+}$ cells in prepubertal porcine testes are a subpopulation of immature spermatogonia. Then, we knocked down *ZBTB16* in enriched porcine immature spermatogonia, and the following RNA-sequencing (RNA-seq) analysis showed that *ZBTB16* knockdown resulted in the manifest transcriptomic change, characterized by downregulation of genes related to spermatogonial self-renewal as well as upregulation of differentiation genes, corroborating ZBTB16 as a factor crucial to porcine spermatogonial self-renewal. Later, by performing a CUT&Tag analysis, we identified the genomic targets of ZBTB16 in porcine immature spermatogonia, and the final integrative analysis for RNA-seq and CUT&Tag data revealed the correlation of ZBTB16 with GDNF and mTOR signaling that facilitates porcine immature spermatogonial self-renewal. Altogether, our results enhance the understanding of molecular mechanisms for spermatogonial self-renewal in pigs, thereby facilitating the *in vitro* culture of porcine SSCs.

## 1. Introduction

Spermatogenesis is a highly productive and intricate process comprised of three consecutive phases, i.e., the mitotic phase (spermatogonial proliferation and differentiation), the meiotic phase (the reductional division of spermatocytes), as well as the spermiogenesis phase (deformation of round spermatids) [1,2]. By spermatogenesis, functional haploid sperm capable of fertilization were produced, thereby sustaining lifelong male fertility. Continual spermatogenesis relies on spermatogonial stem cells (SSCs), a rare population in testes able to self-renew (to maintain sufficient quantities) and differentiate (to become functional mature sperm) [3].

The origin of SSCs is primordial germ cells (PGCs) that have developed into prospermatogonia (also called gonocytes) at birth. After birth, prospermatogonia gradually relocate from the center to the basement membrane of the testicular seminiferous cords/tubules, then becoming undifferentiated spermatogonia composed of a handful of SSCs and the majority of progenitors committed to differentiation [4]. In mice, the migration of prospermatogonia to the basement membrane and their transition into undifferentiated spermatogonia initiate on around post-natal day 3 and finalize by day 7 [4], which is, however, a rather slow and prolonged process that finalizes at some timepoint close to puberty in pigs [5], and because of this, prospermatogonia and undifferentiated spermatogonia present in prepubertal porcine testes can collectively be termed as immature spermatogonia [6–8].

Spermatogonial self-renewal is orchestrated by a battery of transcription factors, of which zinc finger and BTB domain-containing 16 (ZBTB16, also known as PLZF) is the first identified one [9,10]. In mice, the expression of ZBTB16 was first detected in E17.5 germ cells and culminated in type An undifferentiated spermatogonia at approximately

* Corresponding author.
** Corresponding author.
*E-mail addresses:* pengwang@nxmu.edu.cn (P. Wang), y.zheng@nwafu.edu.cn (Y. Zheng).

https://doi.org/10.1016/j.theriogenology.2025.01.026
Received 18 July 2024; Received in revised form 26 January 2025; Accepted 28 January 2025
Available online 30 January 2025

one week after birth [10]. It has further been demonstrated that *Zbtb16*-deficient murine undifferentiated spermatogonia failed to colonize the recipient testis after transplantation [9,10], suggesting that ZBTB16 is crucial to maintenance and self-renewal of murine undifferentiated spermatogonia including SSCs. In addition, a study showed that overexpression of ZBTB16 led to cell cycle arrest at the G1 to S transition and suppressed the expression of genes related to proliferation [11], suggesting a growth inhibitory role of ZBTB16. ZBTB16 has also been reported to be capable of repressing spermatogonial differentiation by directly repressing the transcription of *KIT* [12], supporting the essential role for ZBTB16 in balancing murine spermatogonial self-renewal and differentiation [13]. Subsequent studies showed the expression of ZBTB16 in spermatogenic subpopulations from pigs, cattle, sheep, goats or equids [14–18]. Despite this, the exact expression pattern of ZBTB16 and its regulatory roles in spermatogenic cells from large domestic animals such as pigs, remain enigmatic. Hence, this study aimed to explore the expression pattern of ZBTB16 in porcine testes as well as the regulatory repertoire of ZBTB16 in porcine immature spermatogonia.

## 2. Materials and methods

### 2.1. Animals

Testis samples were obtained from Duroc boars at various ages that had been raised in farms affiliated with Northwest A&F University or with Zhumei Porcine Breeding Corporation, Henan, China. Specifically, for immunohistochemistry, we collected four ages (days 7, 30, 70, and 90) of testes from 12 Duroc boars, with testis samples at each age harvested from three littermates, and for *in vitro* experiments, 16 testes from eight 7-day-old Duroc piglets and eight testes from four 14-day-old Duroc piglets were employed. Upon castration by professional veterinarians, testis samples were immediately transported to the lab. All animal experimental procedures were approved and carried out in line with the guidelines of the Animal Ethical Committee of Northwest A&F University.

### 2.2. Immunofluorescence staining of testis sections

Testis samples were preserved in pre-chilled DPBS harboring 2 % penicillin-streptomycin and immediately transported to the lab. After removal of tunica albuginea, testis tissues were sectioned into small fragments and fixed in Bouin's solution or 4 % paraformaldehyde (PFA), followed by embedding in paraffin. The embedded testis fragments were then sliced into 5-μm sections using a microtome (Leica, Nussloch, Germany) and dried at 42 °C for 8 h. For immunofluorescence staining, testis sections were deparaffinized and rehydrated with xylene and ethanol, and heat-mediated antigen retrieval was conducted in sodium citrate buffer. Next, testis sections were permeabilized with 0.5 % Triton X-100 for 10 min, and blocked with the commercial blocking buffer (Deeyee, Shanghai, China) at room temperature for 2 h. Then, testis sections were incubated at 4 °C overnight with primary antibodies (shown in Table 1). The isotype mouse or rabbit IgG was used as the negative control. After washing on the next day, testis sections were incubated with the corresponding secondary antibodies (shown in Table 1) at 4 °C for 2 h. Finally, testis sections were stained with DAPI at room temperature for 5 min, and visualized and quantified under a microscope. To quantify positive cells per seminiferous cord/tubule cross-section, 50 randomly selected round cord/tubule cross-sections were analyzed per animal, and testis sections from three littermates at each age were analyzed, as previously described [19,20].

### 2.3. Isolation and enrichment of porcine immature spermatogonia

To isolate and enrich porcine immature spermatogonia, testis samples were collected from piglets aged 7–14 days. Specifically, 16 testes from eight 7-day-old Duroc piglets and eight testes from four 14-day-old Duroc piglets were employed. Upon removal from the body, the tunica albuginea was discarded, and the testes were cut into ~2 $mm^3$ fragments and incubated with type IV collagenase (Thermo Fisher Scientific) dissolved in DMEM (CORNING) at 37 °C for 15 min, followed by centrifugation and multiple wash to remove interstitial cells and erythrocytes. The pellet harboring seminiferous cords/tubules was then incubated with 0.25 % trypsin-EDTA (Solarbio) at 37 °C for 4 min. After termination with FBS (Bioind), the cell suspension was filtered through a 40-μm mesh. Next, the cell pellet was resuspended in the complete medium (DMEM with 10 % FBS), and the cells were counted and seeded at a density of $1.0 \times 10^7$ cells per 10-cm dish for germ cell enrichment by differential plating. Specifically, after seeding and incubation at 37 °C in an atmosphere of 5 % $CO_2$ in air for 1 h, the supernatant harboring germ cells was collected and transferred to new 10-cm culture dishes for the additional 2-h incubation. The supernatant harboring germ cells was repeatedly collected and transferred to new 10-cm culture dishes for overnight incubation. The next day, the floating as well as loosely attached cells, which were enriched with immature spermatogonia, were collected for downstream experiments.

**Table 1**
The antibody information.

| Antibody | Species Source | Supplier | Identifier | Dilution IHC | Dilution ICC |
|---|---|---|---|---|---|
| DBA | Mouse | Vector Laboratories | RL-1032-2 ab8189 | 1:100 | |
| UCHL1 | | Abcam | | 1:500 | |
| Ki67 | Mouse | Abcam | ab279653 | 1:200 | |
| SALL4 | Mouse | Abcam | ab57577 | 1:200 | |
| ZBTB16 | Rabbit | Santa Cruz | sc-22839 | 1:100 | 1:100 |
| UCHL1 | Rabbit | Proteintech | 14730-1-AP | | 1:500 |
| VASA | Rabbit | Abcam | ab13840 | | 1:500 |
| AF488 | Donkey anti-rabbit | Yeasen | 34206ES60 | 1:300 | 1:300 |
| AF594 | Goat anti-mouse | Yeasen | 33212ES60 | 1:300 | 1:300 |

IHC: immunohistochemistry; ICC: immunocytochemistry.

### 2.4. Immunofluorescence staining of cells

Immunofluorescence staining was carried out on 4 % PFA-fixed cytospin slides of cells before or after differential plating. The cells were permeabilized with 0.5 % Triton X-100 for 10 min, and then blocked with the commercial blocking buffer (Deeyee, Shanghai, China) at 4 °C for 2 h. After blocking, the cells were incubated at 4 °C overnight with primary antibodies (shown in Table 1). The isotype rabbit IgG was used as the negative control. After washing on the next day, the cells were incubated with the corresponding secondary antibody (shown in Table 1) at 4 °C for 2 h. Finally, the cells were stained with DAPI at room temperature for 5 min, and visualized and quantified under a microscope. To determine the efficiency of cell enrichment in each independent experiment, 900 cells from three slides (300 cells per slide) were randomly selected and analyzed in each group.

### 2.5. Cell culture

The enriched porcine immature spermatogonia were seeded into 6-well plates coated with laminin (20 μg/mL; Thermo Fisher Scientific) at the density of $1.0 \times 10^6$ cells per well, and then cultured in the complete medium comprising DMEM (high glucose; Solarbio), 1 % FBS (Bioind), 1 × non-essential amino acids (Thermo Fisher Scientific) and 1 × penicillin-streptomycin (Solarbio). The culture was maintained at 37 °C in an atmosphere of 5 % $CO_2$ in air.

### 2.6. ZBTB16 knockdown in enriched porcine immature spermatogonia

The siRNA sequence targeting *ZBTB16* (5′-GCGGAAAGCGGTTCCTGGATAGTTT-3′) and a scramble sequence (5′-GCGGATAGCGATTCATGGATAGGTT-3′) were validated and cloned into the shRNA expression vector pGreenPuro (System Biosciences), following the manufacturer's instructions. To produce lentiviruses, the lentiviral backbone (pMD2.G), the packaging vector (psPAX2) and the constructed transfer vector (pGreenPuro) were co-transfected into HEK293T cells, using a liposome-based transfection reagent (Yeasen). After transfection for 16 h, the cells were refreshed and maintained for additional 48 h. The supernatant was collected and concentrated by using a lentivirus concentration reagent (Biodragon), following the manufacturer's instructions. The concentrated lentiviruses were then used for lentiviral transduction. In brief, the lentiviruses at a MOI of 30, in conjunction with 10 μg/mL polybrene (MedChemExpress), were added to 6-well plates seeded with the enriched porcine immature spermatogonia, followed by "spinfection" [21] and incubation for additional 16 h. Subsequently, the cells were refreshed and cultured for 48 h, and then harvested for downstream experiments.

### 2.7. qPCR

Total RNAs were extracted from the lentiviral transduced cells using Trizol (Thermo Fisher Scientific). After DNase (TIANGEN) treatment to remove genomic DNAs, RNAs were reversely transcribed using 5 × Smart RT Master Mix (DeeYee), and the synthesized cDNAs were used as templates for PCR. For the qPCR analysis, an IQ5 platform (Bio-Rad) was utilized, and reactions were performed in a 25-μL volume system harboring SYBR Green II PCR Mix (Takara). The reactions were performed in triplicates in each independent experiment, and three independent experiments were performed. The data were analyzed using the $2^{-\Delta\Delta Ct}$ method, using *HPRT1* as the reference gene. The information on primer sequences and corresponding qPCR products is provided in Table 2.

### 2.8. RNA-seq

Total RNAs were extracted from duplicates of *ZBTB16*-knockdown and control cells using Trizol (Thermo Fisher Scientific). The extracted RNAs were then treated with DNase (TIANGEN) to remove genomic DNAs. Subsequently, the RNA samples were sent to the Frasergen Corporation (Wuhan, China) for mRNA-seq library construction, and the libraries were sequenced using the MGI high-throughput sequencing platform. Raw reads were filtered using the SOAPnuke (v2.1.0) software to obtain clean reads that were then aligned to the pig genome (Sscrofa 11.1) using HISAT2 (v2.2.1). RSEM (v1.3.3) was used to count the number of reads mapped to each transcript in each sample and to convert them to FPKM, thereby obtaining the expression levels of genes and transcripts. Finally, the DESeq2 algorithm was employed with a loose cutoff (false discovery rate <0.05) to filter differentially expressed genes (DEGs). Gene Ontology (GO) and Kyoto Encyclopedia of Genes and Genomes (KEGG) analyses were performed using Metascape (http://metascape.org). The raw and processed RNA-seq datasets have been submitted to the NCBI GEO database and would be available under the accession number GSE271152.

**Table 2**
Primer and qPCR product information.

| Gene | Primer sequence (5′–3′) | Product size (bp) |
|---|---|---|
| *TRAF2* | F: ATCGAAGCCCTGAGCAACAA<br>R: TCCAGATGAAGACGCCATCG | 130 |
| *DDIT4* | F: AACTGCTCTAGCTGCGTCTTC<br>R: CGACGAGAAGCGATCCCAAA | 105 |
| *IFIT2* | F: TGGGACAGAGGAGGATTTCTG<br>R: GAGTTCTTTGTGGTCTCACTTTTAG | 186 |
| *KIT* | F: CATGCACCAATGAAGGCGGTT<br>R: CAGCCCGTGAGGGAGTAATT | 166 |
| *PABPC1* | F: TCCAAGAAGGAACCAAGAGACC<br>R: CGCAGAGGGACAAAAATCAAC | 160 |
| *IGF1* | F: CACATCACATCCTCTTCG<br>R: CTGGAGCCGTACCCTGTG | 173 |
| *ID2* | F: CAGAACAAGAAGGTGAGCAAGATGG<br>R: TGATGTCCGTATTTAGGGTGGTCAG | 169 |
| *CUX1* | F: GAGGGAGGCAGAGACCTTGA<br>R: TATGGCCTGCTCCACGTCC | 100 |
| *HPRT1* | F: CCCAGCGTCGTGATTAGTG<br>R: CACAGAGGGCTACGATGTGA | 184 |

### 2.9. CUT&Tag

A CUT&Tag analysis for ZBTB16 was performed on duplicates of the enriched porcine immature spermatogonia. Specifically, around 100,000 cells were harvested and centrifuged for 3 min at 600×*g* at room temperature. The cells were then washed twice in 300 μL Wash Buffer (20 mM HEPES, pH 7.5; 150 mM NaCl; 0.5 mM Spermidine; 1 × Protease inhibitor cocktail) by gentle pipetting. The 10 μL activated concanavalin A-coated magnetic beads were added to each sample and incubated at room temperature for 10 min. The supernatant was then removed and the bead-binding cells were resuspended in 50 μL Dig-wash Buffer (20 mM HEPES, pH 7.5; 150 mM NaCl; 0.5 mM Spermidine; 1 × Protease inhibitor cocktail; 0.05 % Digitonin) harboring 2 mM EDTA and the primary antibody rabbit anti-ZBTB16 (1: 50; Santa Cruz, sc-22839). Incubation with the primary antibody was performed on a rotating platform for 2 h at room temperature, and the liquid was then removed from the magnet stand. The secondary antibody goat anti-rabbit IgG (1: 50; Proteintech, B900210) was diluted in 50 μL Dig-Wash buffer and the cells were incubated at room temperature for 1 h. To construct the negative control library (IgG), only the secondary antibody was added. Subsequently, using the magnet stand, the cells were washed twice (1 min for each) in 500 μL Dig-Wash buffer to remove unbinding antibodies. A dilution (1: 200) of the pG-Tn5 adapter complex (about 0.04 μM) was prepared in Dig-300 Buffer (0.01 % Digitonin; 20 mM HEPES, pH 7.5; 300 mM NaCl; 0.5 mM Spermidine; 1 × Protease inhibitor cocktail). After removal of the liquid, 100 μL were added to the cells with gentle vortex, and they were incubated with pG-Tn5 at room temperature for 1 h. Cells were washed twice (1 min for each) in 500 μL Dig-300 Buffer to remove the unbinding pG-Tn5 protein. Next, cells were resuspended in 300 μL Tagmentation buffer (10 mM $MgCl_2$ in Dig-300 Buffer) and incubated at 37 °C for 1 h. To terminate tagmentation, 10 μL 0.5M EDTA, 3 μL 10 % SDS and 2.5 μL 20 mg/mL Proteinase K were added to the 300 μL samples, and they were further incubated at 55 °C for 1 h, purified using phenol-chloroform-isoamyl alcohol and ethanol, washed with 100 % ethanol and suspended in water.

The DNAs were amplified by PCR reaction as follows: 3 min at 72 °C and 30 s at 98 °C, followed by 16 cycles of 15 s at 98 °C and 30 s at 60 °C and 30 s at 72 °C, with a final extension at 72 °C for 3 min. Post-PCR cleanup was performed by adding NovoNGS DNA clean beads, and libraries were incubated with beads for 15 min at room temperature, gently washed twice in 80 % ethanol, and eluted in 20 μL TE buffer. The DNA fragments were used for stranded DNA library preparation. Then, the library was detected by agarose electrophoresis, quantified using Qubit 2.0, and sequenced on an Illumina NovaSeq 6000 platform in the Frasergen Corporation (Wuhan, China). The original double-ended sequencing data harbored junction information, low-quality and undetected bases (represented by N). Therefore, this interference information was removed by fine filtering methods (FastQC (0.11.9) and Trimmomatic (v0.39) software). After quality control, the clean data were mapped to the reference genome sequence by Bowtie2, and the reads on the comparison were further screened by Samtools (V1.12) and Picard (v2.25.6) software to remove PCR redundancy, low quality and organelle comparisons, and the final effective data were obtained for subsequent analyses. Next, peak calling was performed on the final valid data

using MACS3 (v3.0.0a6) software. Based on statistical methods, significantly enriched peaks were obtained. The peak in each sample was annotated by ChIPseeker to find the gene associated with the peak (the gene represented by the TSS most adjacent to the peak center), and the base of the peak-associated gene was determined by clusterProfiler. The distribution of CUT&Tag signals in gene body and their flanking 3 kb regions were plotted by R script. Later, the peaks detected between parallel samples in the group were merged to obtain the peaks in the group. DiffBind was used to analyze the difference peak (DP) between groups, and the signal values of DP in each sample between groups were clustered. Then, ChIPseeker was used to assign the DP results between groups to the location of the genome and to find the genes associated with DP (the genes represented by the TSS most adjacent the DP center). Finally, ClusterProfiler was used to perform GO and KEGG annotation and enrichment analyses on the gene sets of DP-associated genes. The raw and processed CUT&Tag datasets have been submitted to the NCBI GEO database and would be available under the accession number GSE271393.

### 2.10. Data analysis

All experimental data were presented as the mean ± SEM from three littermates or three independent experiments. Statistical significances between two or more groups were determined by the Student's t-test or by one-way ANOVA in combination with the LSD method, respectively. Statistically significant differences were defined when $P < 0.05$. *: $P < 0.05$; **: $P < 0.01$.

## 3. Results

### 3.1. Localization of ZBTB16 in porcine testes and its co-staining with spermatogonial/proliferative markers

First, we collected testes from four ages (days 7, 30, 70 and 90) of prepubertal Duroc boars, and conducted co-staining for ZBTB16 and spermatogonial/proliferative markers on testis section. *Dolichos biflorus agglutinin* (DBA) is a lectin with specific affinity for primitive spermatogenic cells (i.e., prospermatogonia and early undifferentiated spermatogonia) in neonatal boars [5,22]. By co-staining for ZBTB16 and DBA (Fig. 1A), we identified ZBTB16 staining exclusively in germ cells with round morphology and large nuclei, and that the number of ZBTB16$^+$ cells per tubule cross-section increased with age. Specifically, the number of ZBTB16$^+$ cells per tubule cross-section was 2.48 ± 0.08 on day 7, and it went up to 3.3 ± 0.02 on day 90. In contrast, the number of ZBTB16$^+$DBA$^+$ cells per tubule cross-section fluctuated at four ages of porcine testes. On day 7, the number of ZBTB16$^+$DBA$^+$ cells per tubule cross-section was 0.64 ± 0.04, and it grew to 1.14 ± 0.02 on day 70 but reduced to 0.46 ± 0.06 on day 90, due to the sharp decline of DBA$^+$ cells at this age (Fig. 1B). By quantification of ZBTB16$^+$DBA$^+$ cells, we also found 41.1 ± 1.56 % of ZBTB16$^+$ cells per tubule-cross section positive for DBA on day 7, and this percentage increased to 48.1 ± 1.84 % on day 70 but decreased to 19.4 ± 1.84 % on day 90. On day 7, 52.0 ± 2.83 % of DBA$^+$ cells per tubule-cross section were positive for ZBTB16, with this percentage rising to 71.95 ± 7.43 % on day 30 and stabilizing from that point onwards (Fig. 1C). These results suggest that ZBTB16 partially co-localizes with DBA in porcine testes.

The transcription factor Sal-like protein 4 (SALL4) is expressed in early immature spermatogonia in prepubertal pigs [23]. The result of ZBTB16 and SALL4 co-staining (Fig. 2A) showed that the numbers of both ZBTB16$^+$ and SALL4$^+$ cells per tubule cross-section increased with age, in particular after day 70 (Fig. 2B). On day 7, 82.56 ± 4.79 % of SALL4$^+$ cells per tubule cross-section were positive for ZBTB16. This percentage remained stable by day 70 but sharply decreased on day 90, due to the rapid rise of SALL4$^+$ cells at this age (Fig. 2C). Notably, almost all ZBTB16$^+$ cells overlapped with SALL4$^+$ cells before day 90. These results suggest that ZBTB16 largely co-localizes with SALL4 in porcine testes.

Ubiquitin C-terminal hydrolase L1 (UCHL1, also known as PGP9.5) is a specific marker for porcine immature spermatogonia [5,15]. Co-staining for ZBTB16 and UCHL1 (Fig. 3A) revealed that the numbers of both UCHL1$^+$ and ZBTB16$^+$UCHL1$^+$ cells per tubule cross-section increased with age (Fig. 3B), and that almost all ZBTB16$^+$ cells stained

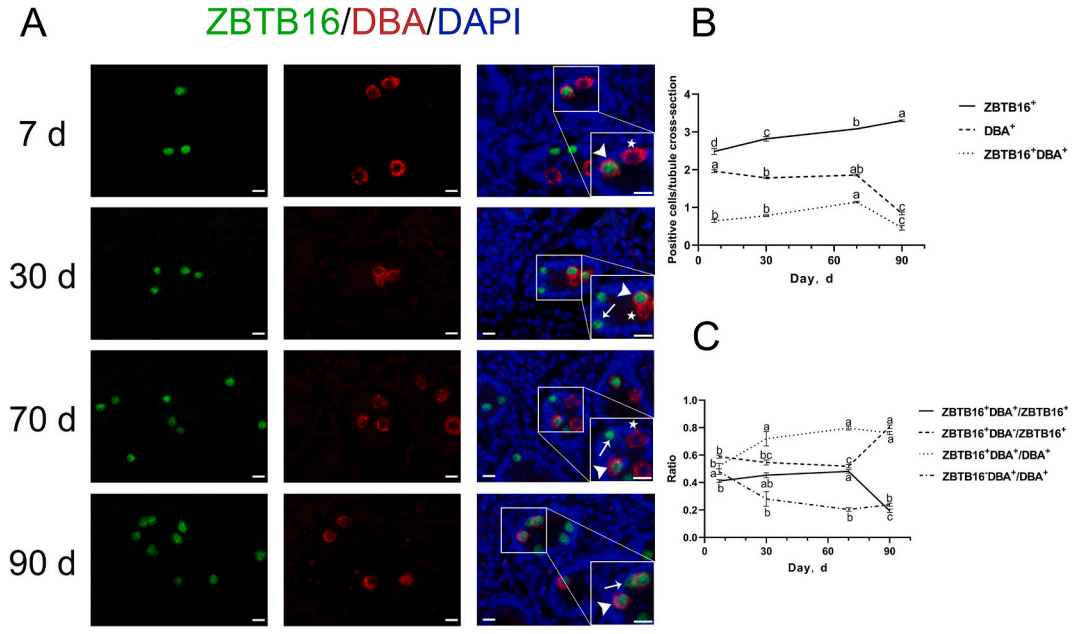


**Fig. 1.** Co-staining and quantification of ZBTB16$^+$DBA$^+$ cells on porcine testis sections. (A) Co-staining for ZBTB16 and DBA on testis sections from four ages of boars. Arrows, arrowheads and asterisks denote ZBTB16$^+$DBA$^-$, ZBTB16$^+$DBA$^+$ and ZBTB16$^-$DBA$^+$ cells, respectively. Bar = 10 μm. (B) Quantification of ZBTB16$^+$DBA$^+$ cells per tubule cross-section in four ages of porcine testes. (C) The ratios of ZBTB16$^+$DBA$^\pm$ to ZBTB16$^+$ and ZBTB16$^\pm$DBA$^+$ to DBA$^+$ cells per tubule cross-section in four ages of porcine testes. Data are presented as the mean ± SEM of three littermates (n = 3), with 50 round cord/tubule cross-sections counted per animal. Distinct letters refer to significant differences between groups ($P < 0.05$).

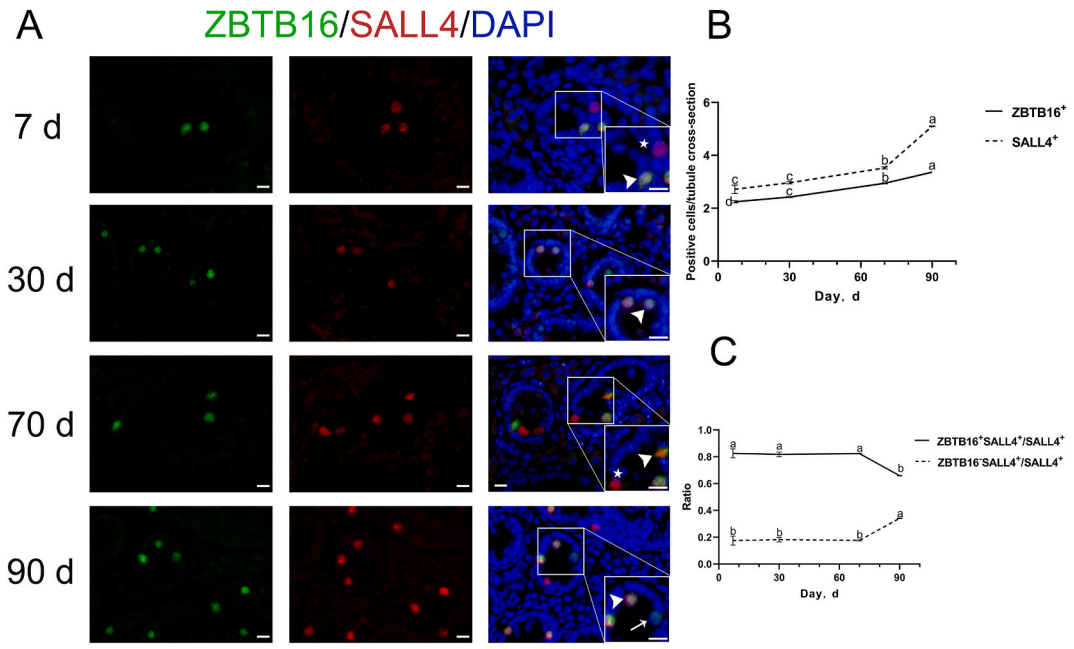


**Fig. 2.** Co-staining and quantification of ZBTB16$^{+}$SALL4$^{+}$ cells on porcine testis sections. (A) Co-staining for ZBTB16 and SALL4 on testis sections from four ages of boars. Arrows, arrowheads and asterisks denote ZBTB16$^{+}$SALL4$^{-}$, ZBTB16$^{+}$SALL4$^{+}$ and ZBTB16$^{-}$SALL4$^{+}$ cells, respectively. Bar = 10 μm. (B) Quantification of ZBTB16$^{+}$ and SALL4$^{+}$ cells per tubule cross-section in four ages of porcine testes. (C) The ratios of ZBTB16$^{\pm}$SALL4$^{+}$ to SALL4$^{+}$ cells per tubule cross-section in four ages of porcine testes. Data are presented as the mean ± SEM of three littermates (n = 3), with 50 round cord/tubule cross-sections counted per animal. Distinct letters refer to significant differences between groups ($P < 0.05$).

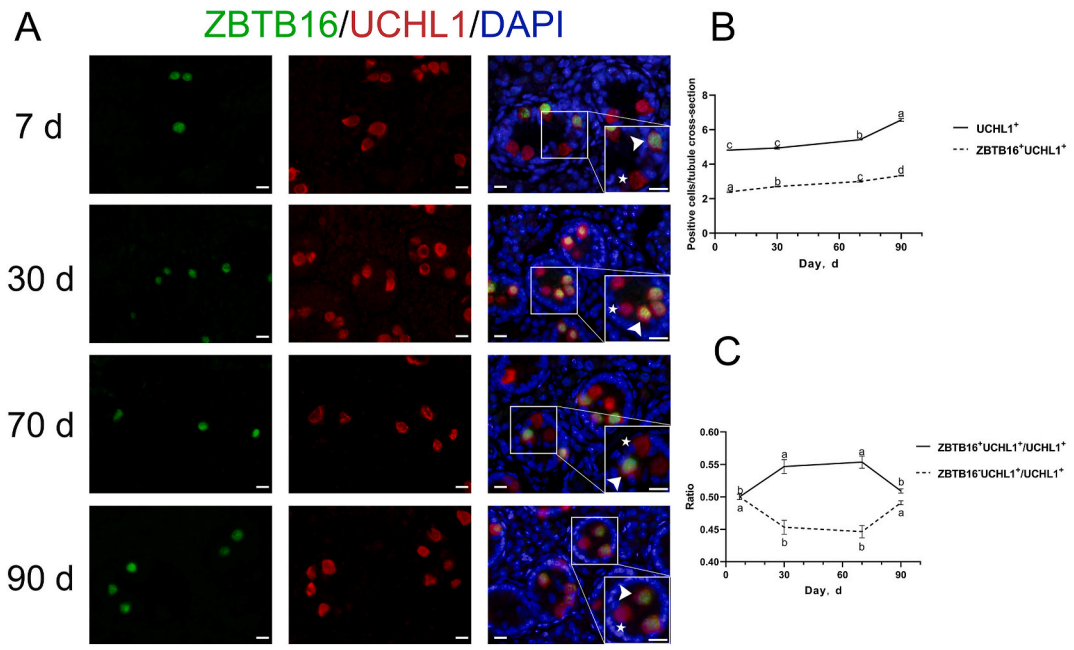


**Fig. 3.** Co-staining and quantification of ZBTB16$^{+}$UCHL1$^{+}$ cells on porcine testis sections. (A) Co-staining for ZBTB16 and UCHL1 on testis sections from four ages of boars. Arrowheads and asterisks denote ZBTB16$^{+}$UCHL1$^{+}$ and ZBTB16$^{-}$UCHL1$^{+}$ cells, respectively. Bar = 10 μm. (B) Quantification of ZBTB16$^{+}$UCHL1$^{+}$ cells per tubule cross-section in four ages of porcine testes. (C) The ratios of ZBTB16$^{\pm}$UCHL1$^{+}$ to UCHL1$^{+}$ cells per tubule cross-section in four ages of porcine testes. Data are presented as the mean ± SEM of three littermates (n = 3), with 50 round cord/tubule cross-sections counted per animal. Distinct letters refer to significant differences between groups ($P < 0.05$).

positive for UCHL1. On day 7, 50.0 ± 0.59 % of UCHL1$^{+}$ cells per tubule cross-section co-stained with ZBTB16. This percentage grew to 54.67 ± 1.51 % on day 30, stabilized between days 30 and 70, and declined to 50.92 ± 0.45 % on day 90, due to the sharp increase of UCHL1$^{+}$ cells at this age (Fig. 3C). These results suggest that ZBTB16$^{+}$ cells are a subpopulation of UCHL1$^{+}$ cells, corroborating ZBTB16 as a marker for porcine immature spermatogonia.

We also carried out co-staining for ZBTB16 and Ki67 on testis sections, to explore the proliferative activity of ZBTB16$^{+}$ cells in porcine testes. By co-staining for ZBTB16 and Ki67 (Fig. 4A), we identified that despite the increase of ZBTB16$^{+}$ cells with age, the number of proliferative ZBTB16$^{+}$ cells per tubule cross-section generally remained stable.

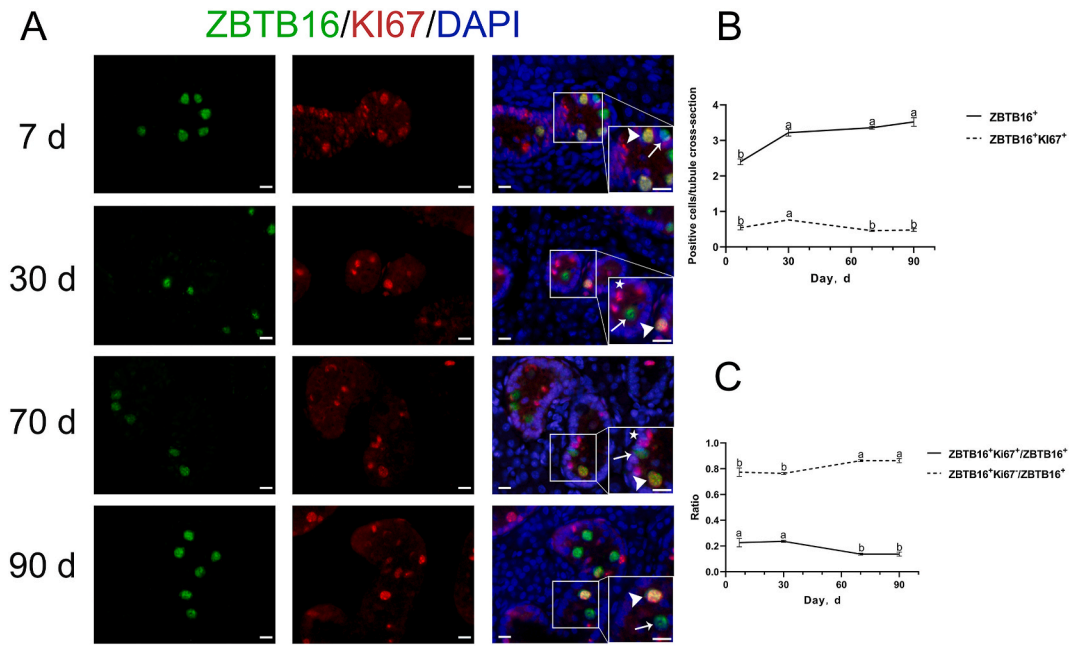


**Fig. 4.** Co-staining and quantification of ZBTB16$^{+}$Ki67$^{+}$ cells on porcine testis sections. (A) Co-staining for ZBTB16 and Ki67 on testis sections from four ages of boars. Arrows, arrowheads and asterisks denote ZBTB16$^{+}$Ki67$^{-}$, ZBTB16$^{+}$Ki67$^{+}$ and ZBTB16$^{-}$Ki67$^{+}$ cells, respectively. Bar = 10 μm. (B) Quantification of ZBTB16$^{+}$Ki67$^{+}$ cells per tubule cross-section in four ages of porcine testes. (C) The ratios of ZBTB16$^{+}$Ki67$^{\pm}$ to ZBTB16$^{+}$ cells per tubule cross-section in four ages of porcine testes. Data are presented as the mean ± SEM of three littermates (n = 3), with 50 round cord/tubule cross-sections counted per animal. Distinct letters refer to significant differences between groups ($P < 0.05$).

Specifically, the number of ZBTB16$^{+}$Ki67$^{+}$ cells per tubule cross-section was 0.54 ± 0.06 on day 7, with a rise to 0.76 ± 0.01 on day 30, and it dropped to 0.46 ± 0.02 on day 70 and stabilized thereafter (Fig. 4B). On day 7, 22.6 ± 3.3 % of ZBTB16$^{+}$ cells per tubule cross-section were positive for Ki67, and this percentage reduced to 13.7 ± 0.8 % on day 70 and then remained stable (Fig. 4C). These results suggest the dynamic proliferative activity of ZBTB16$^{+}$ cells during porcine testicular development.

### 3.2. *Downregulation of ZBTB16 triggered the manifest transcriptomic change in porcine immature spermatogonia*

To probe the molecular mechanism mediated by ZBTB16 in porcine immature spermatogonia, we subsequently isolated and enriched immature spermatogonia from neonatal piglets, and knocked down *ZBTB16* in the collected cell fraction, followed by an RNA-seq analysis. To be more specific, we collected testes from neonatal piglets aged 7–14 days, and employed an established collagenase-trypsin dissociation procedure to obtain the single-cell suspension comprising immature spermatogonia and somatic cells. The optimized differential plating approach was then applied for spermatogonial enrichment. After differential plating, immature spermatogonia with round morphology and large nuclei were efficiently enriched in the cell fraction (Fig. 5A), which was confirmed by immunofluorescence staining for spermatogonial/germ cell markers (ZBTB16, UCHL1 or VASA, Fig. 5B and C). Next, we knocked down *ZBTB16* in the enriched porcine immature spermatogonia, by introducing a *ZBTB16*-shRNA expression vector into the cells through optimized lentiviral transduction, and performed an RNA-seq analysis on duplicates of *ZBTB16*-knockdown and control cells at 48 h post-lentiviral transduction. Both the principal component analysis (PCA) plot (Fig. 5D) and the Pearson correlation analysis (Fig. 5E) uncovered the manifest transcriptomic change in porcine immature spermatogonia induced by *ZBTB16* knockdown. Given the modest downregulation of *ZBTB16* as well as the presence of somatic cells in the cell fraction for RNA-seq, we used a loose cutoff (false discovery rate <0.05) to identify differentially expressed genes (DEGs) [24], with an aim to obtain a thorough list of genes potentially modulated by ZBTB16 in porcine immature spermatogonia. As a consequence, we identified 5931 DEGs consisting of 2898 upregulated and 3033 downregulated ones (Table S1), as shown by the volcano plot (Fig. 5F). As expected, knockdown of *ZBTB16* downregulated genes in relation to spermatogonial self-renewal, such as *DDIT4*, *IFIT2*, *AKT1* and *WNT9A*, and upregulated differentiation genes such as *KIT*, *MTOR* and *DAZL* (Fig. 5G–Table S1). It has been reported that ZBTB16 can repress the mTOR signaling that promotes spermatogonial differentiation in mice [25,26]. Consistently, genes involved in the mTOR signaling, such as *FNIP2*, *CASTOR2*, *STRADB* and *CLIP1*, were upregulated by *ZBTB16*-knockdown, as revealed by the RNA-seq data (Fig. 5G–Table S1). The Gene Ontology (GO) analysis uncovered that upregulated genes by *ZBTB16*-knockdown were related to nucleus, cellular process, intracellular anatomical structure, binding and organelle, whilst downregulated genes fell in terms such as intracellular anatomical structure, cytoplasm, organelle, metabolic and cellular processes (Fig. 5H–Table S2). The Kyoto Encyclopedia of Genes and Genomes (KEGG) pathway analysis disclosed that upregulated genes by *ZBTB16*-knockdown were involved in regulation of actin cytoskeleton, focal adhesion, endocytosis, axon guidance and MAPK signaling pathway, whereas downregulated genes were enriched with pathways such as ribosome, oxidative phosphorylation, thermogenesis, spliceosome and protein processing in endoplasmic reticulum (Fig. 5I–Table S3). We additionally conducted a qPCR analysis for some known ZBTB16 target genes (Fig. 5J), and found the qPCR result generally in concert with the RNA-seq data, thereby validating our RNA-seq analysis.

### 3.3. *The binding sites of ZBTB16 and the assigned genes in porcine immature spermatogonia*

The aforementioned RNA-seq data showed the DEGs upon *ZBTB16* knockdown, but the ZBTB16 target genes, as well as the signaling directly orchestrated by ZBTB16 in porcine immature spermatogonia, remain elusive. To acquire more knowledge in this respect, we first

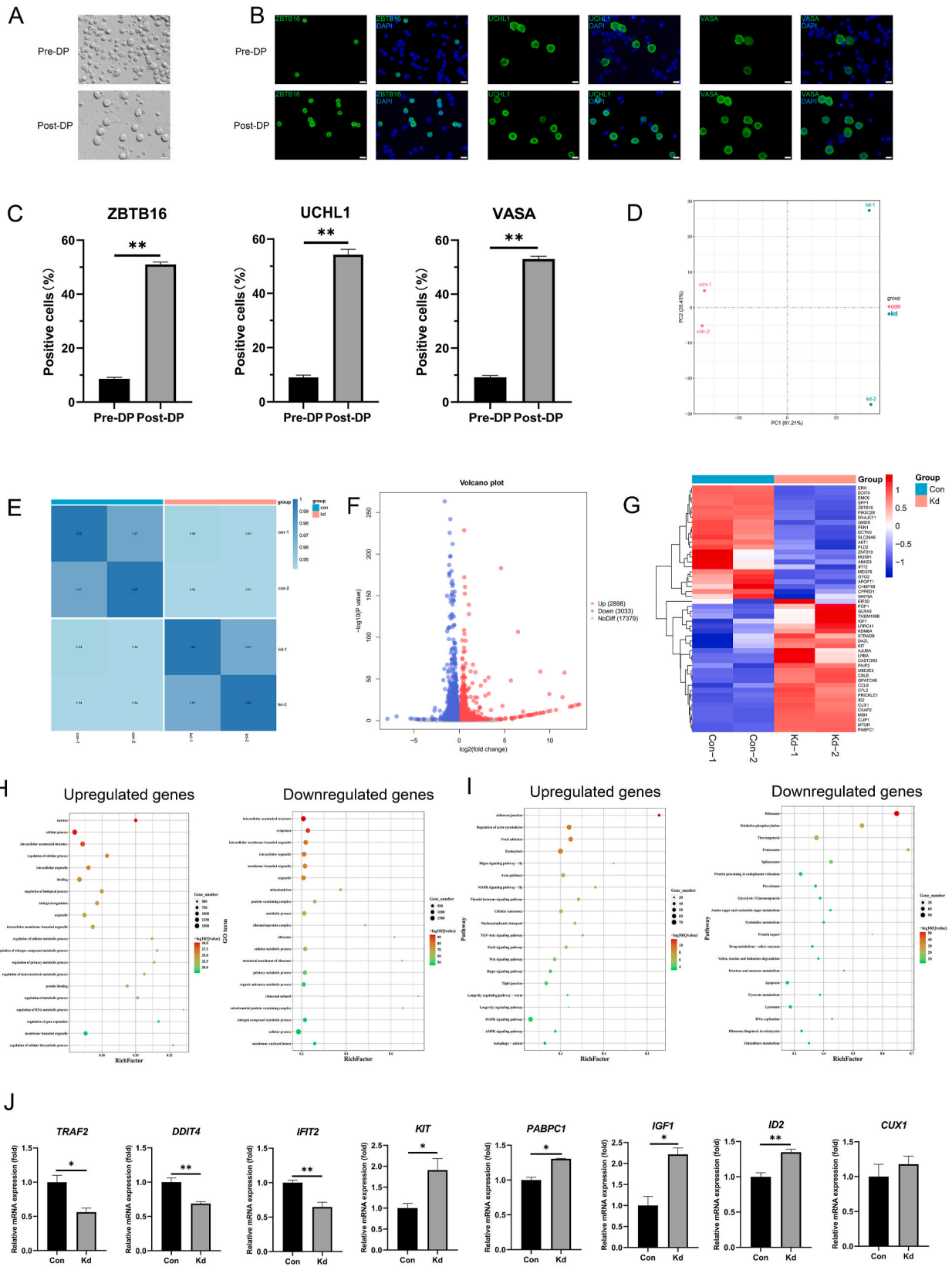


**Fig. 5.** Downregulation of *ZBTB16* triggered the manifest transcriptomic change in porcine immature spermatogonia. (A) The single-cell suspension pre/post-differential plating (DP). Bar = 10 μm. (B) ZBTB16, UCHL1 and VASA immunofluorescence staining on cells pre/post-DP. Bar = 10 μm. (C) The percentages of ZBTB16$^+$, UCHL1$^+$ and VASA$^+$ cells pre/post-DP. (D and E) The PCA plot (D) and the Pearson correlation analysis (E) illustrating the manifest transcriptomic change in porcine immature spermatogonia upon *ZBTB16* knockdown. (F and G) The volcano plot (F) and the heatmap (G) showing the up- and down-regulated genes. (H and I) GO (H) and KEGG pathway (I) analyses of up- and down-regulated genes. (J) The qPCR analysis of some known ZBTB16 target genes in *ZBTB16*-knockdown and control cells. Data are presented as the mean ± SEM of three independent experiments (n = 3). *: $P < 0.05$; **: $P < 0.01$.

analyzed the protein-protein interaction (PPI) between porcine ZBTB16 and other proteins by employing STRING [27,28], and found that ZBTB16 interacts with proteins relevant to both spermatogonial self-renewal (e.g., UCHL1, UTF1, NANOS2, GDNF, GFRA1, POU5F1 and ETV5) and differentiation (e.g., KIT, STRA8, RARA, SYCP3, DDX4, DAZL, Fig. 6A). Then, we performed a CUT&Tag analysis for ZBTB16 on duplicates of the enriched porcine immature spermatogonia, to identify the binding sites of ZBTB16 and the assigned genes. The CUT&Tag data showed that ZBTB16-binding site peaks were enriched in regions flanking transcription start sites (TSS) but not in gene body regions (regions between TSS and transcription end sites, TES, Fig. 6B). Comparison of the peaks in each sample showed strong correlation between duplicates (Fig. 6C), demonstrating the specificity of ZBTB16-binding sites and the reliability of our CUT&Tag data. ZBTB16 bound 10,289 and 7312 sites in samples 1 and 2, respectively, with 5468 sites shared between two samples (Fig. 6D–Table S4). The majority (78.47 %) of shared binding sites were present in regions adjacent to promoters, whereas a small fraction was present in untranslated regions (UTR), exons, introns and distal intergenic regions (Fig. 6E), suggesting that ZBTB16 may act as a transcription activator or repressor to regulate gene expression in porcine immature spermatogonia, consistent with that in mice [26,29,30]. To predict the ZBTB16 regulatory targets, we next assigned the binding sites to annotated genes, and identified 9126 and 6787 genes mapping to ZBTB16-binding sites in samples 1 and 2, respectively, including 5409 genes mapping to the shared binding sites (Fig. 6F–Table S4), such as those involved in spermatogonial self-renewal and differentiation (*KIT*, *DDIT4*, *CDK2*, *UCHL1*, *ETV5*, *ZFP42*, etc.). To remove the batch effect, only the genes mapping to the shared binding sites were applied to downstream analyses. The GO analysis revealed that these assigned genes were related to transferase complex, RNA splicing and nucleolus, whilst the KEGG pathway analysis showed their involvement in signaling such as ubiquitin-mediated proteolysis, spliceosome and RNA transport (Fig. 6G–Table S5).

### 3.4. *The regulatory repertoire of ZBTB16 in porcine immature spermatogonia*

Finally, to delve into the regulatory repertoire of ZBTB16 in porcine

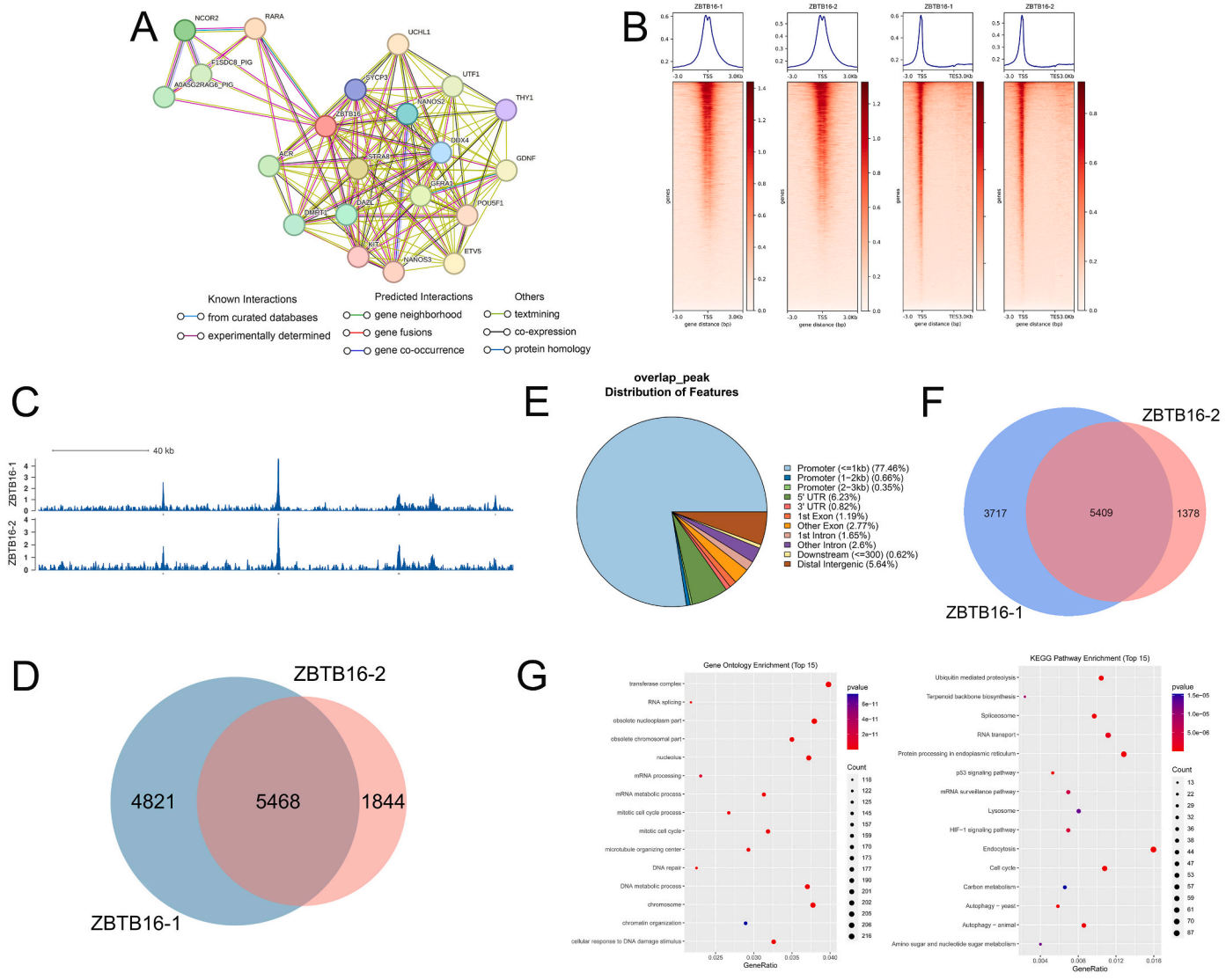


**Fig. 6.** The binding sites of ZBTB16 and the assigned genes in porcine immature spermatogonia. (A) The PPI network between porcine ZBTB16 and other proteins by STRING. (B) The enrichment of ZBTB16-binding site peaks in two samples. (C) Histograms illustrating the abundance of ZBTB16-binding DNA fragments in two samples. (D) The numbers of unique and shared ZBTB16-binding sites in two samples. (E) Composition of the shared ZBTB16-binding site positions in relation to annotated genes. (F) The numbers of annotated genes mapping to unique and shared ZBTB16-binding sites in two samples. (G) GO and KEGG analyses of genes mapping to the shared ZBTB16-binding sites.

immature spermatogonia, we performed an integrative analysis for RNA-seq and CUT&Tag data. Among the DEGs upon *ZBTB16* knockdown (generated by RNA-seq) and the ZBTB16-binding genes (generated by CUT&Tag), we identified 2152 overlapping genes (Fig. 7A), including those related to spermatogonial self-renewal and differentiation (e.g., *DDIT4*, *DNAJB11*, *PCNA* and *KIT*, Fig. 7B–Table S6). Inspection of the ZBTB16-binding sites in these genes revealed the presence of ZBTB16-binding sites in promoters of *DDIT4*, *DNAJB11* and *PCNA*, as well as in introns of *KIT*, with promoters displaying much stronger enrichment of ZBTB16-binding site peaks (Fig. 7C).

It has been reported that the cytokine GDNF can activate the PI3K/AKT pathway through its receptors RET and GFRA1 on mouse undifferentiated spermatogonia, thereby repressing mTORC1 and enhancing the expression of transcription factors related to spermatogonial self-renewal, such as BCL6B, ETV5, LHX1, ID4 and POU3F1 [13,31,32]. In addition, repression of mTORC1 leads to upregulation of ZBTB16, and ZBTB16 *per se* can directly activate genes important to spermatogonial self-renewal [29,31]; therefore, ZBTB16, in an indirect way, participates in GDNF signaling and orchestrates mouse spermatogonial self-renewal. We found that ZBTB16-target genes, which are also related to GDNF signaling in mice, such as *DNAJB11*, *FDPS*, *MATR3*, *FOS*, *OIP5*, *PCNA* and *TAF4B* (Fig. 7B–Table S6), were included in the overlapping genes (i.e., between the DEGs upon *ZBTB16* knockdown and the ZBTB16-binding genes), suggesting that ZBTB16 is also likely to promote porcine immature spermatogonial self-renewal via the crosstalk with GDNF signaling.

Another mechanism for ZBTB16-mediated mouse spermatogonial self-renewal is attained by counteracting the mTORC1 activity. In *ZBTB16*-deficient mouse undifferentiated spermatogonia, the mTORC1 level is markedly elevated, thereby inhibiting the response of undifferentiated spermatogonia to GDNF and the expression of self-renewal genes, eventually depriving undifferentiated spermatogonia of the ability to self-renew and as a consequence, triggering differentiation [33]. We found that ZBTB16-target genes, which are related to mTOR signaling in mice, such as *MTOR*, *MYC*, *HIF1A*, *STRADB*, *MAPK1*, *DDIT4*, *WNT9A* and *HK1* (Fig. 7B–Table S6), were included in the list of overlapping genes. Of these, *Ddit4* has been demonstrated as a pivotal gene activated by ZBTB16 that represses the mTORC1 activity and that enhances the expression of genes involved in GDNF signaling, thereby prompting mouse spermatogonia to self-renew [26]. Hence, it is plausible that ZBTB16 can also facilitate porcine immature spermatogonial self-renewal by modulating the mTOR signaling.

Finally, we performed GO and KEGG analyses for the overlapping genes. The GO analysis showed that these genes fell in terms such as RNA splicing, protein localization to organelle, nucleolus, mRNA metabolic and mitotic cell cycle processes, while the KEGG pathway analysis disclosed their association with signaling such as ubiquitin-mediated proteolysis, thyroid hormone signaling pathway, spliceosome, RNA transport and AMPK signaling pathway (Fig. 7D–Table S6), suggesting the potential regulatory roles of ZBTB16 in numerous biological processes and signaling pathways in porcine immature spermatogonia.

## 4. Discussion

*ZBTB16* is a gene conserved from *C. elegans* to *homo sapiens* and extensively expressed in a variety of tissues. Its encoding protein, ZBTB16, as a potent transcription factor, is principally localized in cell nuclei and plays diverse roles in biological processes and diseases. Previous studies have reported the involvement of ZBTB16 in fate determination of various stem/progenitor cells such as hematopoietic stem cells (HSCs), myeloid progenitors and neuron stem cells (NSCs), balancing stem cell self-renewal and differentiation [13]. Also, ZBTB16 has been demonstrated to orchestrate spermatogonial self-renewal and differentiation in mice, and the underlying molecular mechanisms have been explored [9,10,12,29,34]. Nevertheless, the expression pattern of ZBTB16 and its regulatory repertoire in spermatogenic cells from large domestic animals such as pigs, remain poorly understood.

In this study, we first collected testes from four ages of prepubertal Duroc boars, and conducted co-staining for ZBTB16 and spermatogonial/proliferative markers on testis section. We found ZBTB16 staining exclusively in testicular germ cells with round morphology and large nuclei from all four ages of pigs, suggesting that ZBTB16 is expressed in porcine immature spermatogonia, in line with that in mice [10,35]. The co-staining results further showed that ZBTB16$^+$ cells highly overlapped with DBA$^+$, SALL4$^+$ and UCHL1$^+$ cells, and in particular, that almost all ZBTB16$^+$ cells stained positive for UCHL1, a well-acknowledged marker for porcine immature spermatogonia [5,15]. Together with the result that ZBTB16 staining was discerned in only a portion of UCHL1$^+$ cells, we conclude that ZBTB16$^+$ cells in prepubertal porcine testes are a subpopulation of immature spermatogonia. Besides, by co-staining for ZBTB16 and Ki67, we identified the dynamic proliferative activity of ZBTB16$^+$ cells during porcine testicular development. The underlying molecular mechanisms call for future studies.

To explore the regulatory roles of ZBTB16 in porcine immature spermatogonia, we subsequently performed RNA-seq as well as CUT&Tag analyses. As expected, *ZBTB16* knockdown in enriched porcine immature spermatogonia resulted in the manifest transcriptomic change, characterized by downregulation of genes related to spermatogonial self-renewal as well as by upregulation of differentiation genes, corroborating ZBTB16 as a conserved factor crucial to spermatogonial self-renewal in mammalian species. Also, our results suggest that ZBTB16 is involved in numerous biological processes and signaling pathways in porcine immature spermatogonia. It has been reported that ZBTB16 can promote mouse spermatogonial self-renewal by indirectly participating in the GDNF signaling [13,26], or by repressing the mTORC1 activity via *Ddit4* [26]. Here, we identified that many genes involved in GDNF or mTOR signaling were bound by ZBTB16 and differentially expressed upon *ZBTB16* knockdown, suggesting that ZBTB16 might function similarly in porcine immature spermatogonia.

In this study, we found that *DDIT4* was downregulated upon ZBTB16 knockdown, and that ZBTB16 bound the promoter region of *DDIT4*, suggesting that *DDIT4* might be a direct ZBTB16-target gene involved in porcine immature spermatogonial self-renewal, consistent with that in mice [26,29]. In addition to *DDIT4*, another well-studied ZBTB16-target gene is *KIT*. In mice, ZBTB16 can directly suppress the transcription of *Kit*, thereby inhibiting spermatogonial differentiation [30], and ZBTB16 has been reported to interact with the *Kit* promoter in enriched mouse primary undifferentiated spermatogonia [12]. Yet, in porcine immature spermatogonia, only weak enrichment of ZBTB16-binding site peaks was detected in the *KIT* promoter, and more peaks were identified in introns of *KIT*. This discrepancy might be ascribed to the heterogeneous spermatogonial population, the differential expression patterns of ZBTB16 and the distinct genomes between mice and pigs, suggesting the intricate regulatory repertoire of ZBTB16 in different species and cell categories.

When comparing our ZBTB16 CUT&Tag data (from porcine immature spermatogonia) with the previously reported ZBTB16 ChIP-seq data (from mouse undifferentiated spermatogonia) [29], we found that many ZBTB16-binding genes were shared between mice and pigs, such as *KIT*, *EGR2*, *FOS* and *ETV5*, which are crucial to spermatogonial self-renewal. According to the murine data, *Egr2*, *Fos*, *Etv5* and *Foxo1* were bound by ZBTB16, and they are known to be involved in the GDNF signaling [29,31,36,37]. Of these, *FOXO1*, however, was not identified as a ZBTB16-binding gene in porcine immature spermatogonia, and our RNA-seq data even showed the upregulation of *FOXO1* upon *ZBTB16*-knockdown, suggesting that *FOXO1* might not be directly regulated by ZBTB16, or not involved in the GDNF signaling in porcine immature spermatogonia. In addition, *EGR3* and *EGR4*, two *EGR* family members activated by the MAPK signaling pathway and playing important roles in mouse spermatogonial self-renewal [31], were bound by ZBTB16 in murine but not in porcine spermatogonia, despite *EGR2* identified as a shared ZBTB16-binding gene between mice and pigs,

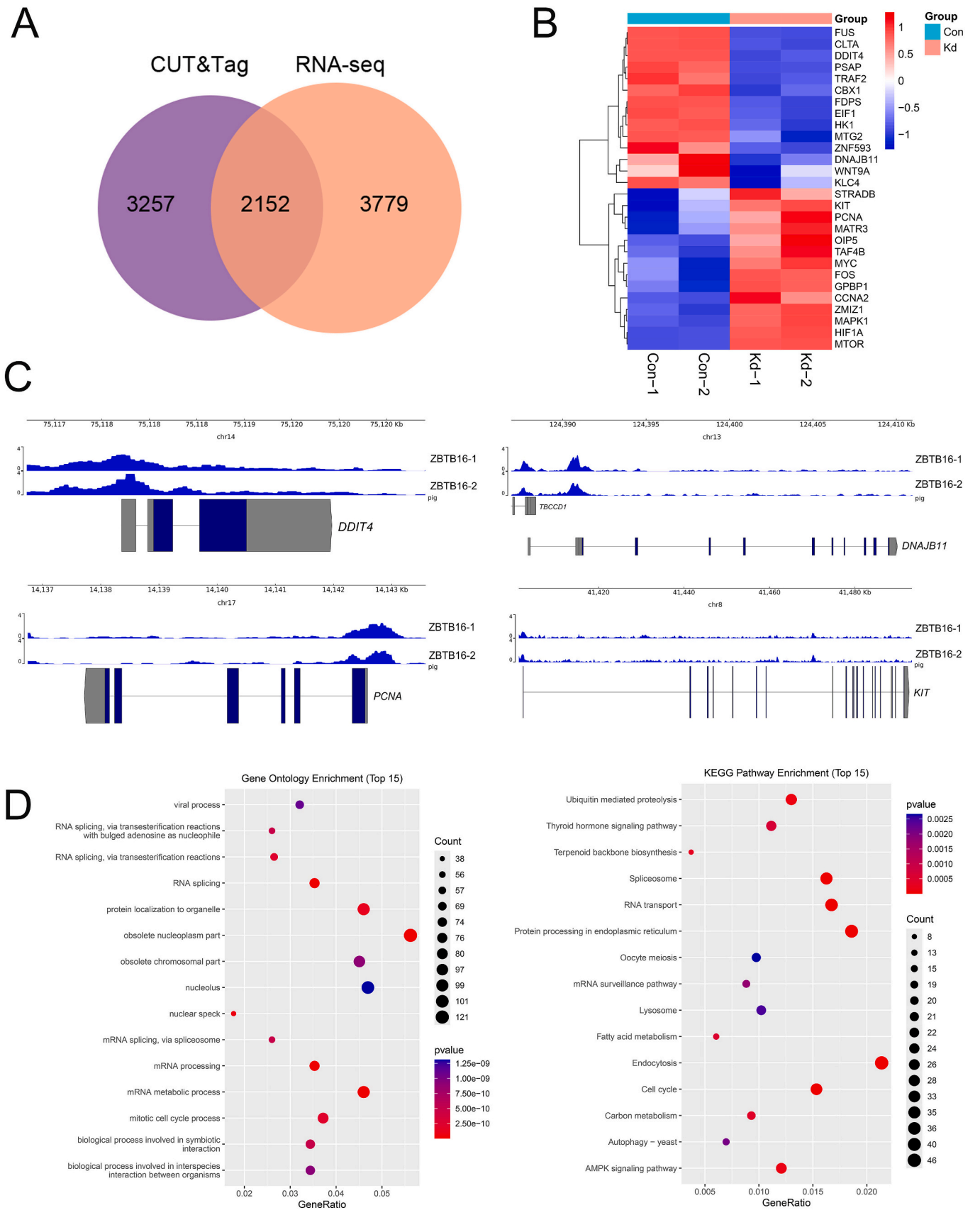


**Fig. 7.** The integrative analysis for RNA-seq and CUT&Tag data. (A) The numbers of DEGs upon *ZBTB16* knockdown, the ZBTB16-binding genes and the overlapping genes. (B) The heatmap showing the expression levels of representative overlapping genes. (C) Histograms illustrating the ZBTB16-binding sites in four overlapping genes. (D) GO and KEGG analyses of overlapping genes.

suggesting differential regulation of the EGR family and even of the MAPK signaling by ZBTB16 in spermatogonia from these two species. Another example is the genes involved in the mTOR signaling, such as *Bcl6b*, *Id4*, *Pou3f1*, *Lhx1* and *Etv5* [29], that were bound by ZBTB16 in mouse spermatogonia. Of these, only *ETV5* and *ID4* fell in the list of ZBTB16-binding genes in porcine spermatogonia, suggesting differential regulation of the mTOR signaling by ZBTB16 in two species. From our perspective, several reasons might underlie this discrepancy. First, there is significant difference between murine and porcine genome, which is likely to result in the differential interaction between ZBTB16 and regulatory elements in genes, thereby modulating distinct genes and signaling pathways in species. Second, the expression patterns of transcription factors (e.g., ZBTB16) and co-regulation factors and their interactions might differ between species. Third, the previously reported ZBTB16 ChIP-seq data were from murine undifferentiated spermatogonia [29], while our ZBTB16 CUT&Tag data were from porcine immature spermatogonia consisting of prospermatogonia and undifferentiated spermatogonia, and the expression of ZBTB16 might differ between spermatogonial subpopulations.

It is also noticeable that some ZBTB16-binding genes in porcine immature spermatogonia were not differentially expressed upon *ZBTB16*-knockdown. A possible reason might be that the assignment of binding peaks to genes was merely predicated on proximity, and because of this, some assignments failed to mirror the authentic regulation. Besides, there might be other transcription factors or regulatory pathways that compensate the functional loss of ZBTB16, eventually stabilizing the expression of ZBTB16-binding genes.

To sum up, we unraveled the exact expression pattern of ZBTB16 and its regulatory repertoire in porcine immature spermatogonia that have so far not been interrogated. Furthermore, by analyzing our data and previous literature, the shared and differential ZBTB16-target genes and signaling between murine and porcine spermatogonia were obtained (Fig. 8). More knowledge in this respect is conducive to the understanding of intricate ZBTB16 regulatory repertoire in different species and cell categories, and more importantly, to the understanding of molecular mechanisms for spermatogonial self-renewal in pigs, thereby facilitating the *in vitro* culture of porcine SSCs.

## CRediT authorship contribution statement

**Youjie Cui:** Writing – original draft, Formal analysis, Data curation. **Wei Liu:** Writing – original draft, Formal analysis, Data curation. **Xueni You:** Data curation. **Wanying Li:** Data curation. **Ruiqi Wu:** Data curation. **Wenxian Zeng:** Supervision, Funding acquisition. **Weijun Pang:** Supervision, Funding acquisition. **Peng Wang:** Supervision, Funding acquisition. **Yi Zheng:** Writing – review & editing, Writing – original draft, Supervision, Methodology, Funding acquisition, Formal analysis, Conceptualization.

## Data availability

All data are included in the article and/or supporting information.

## Funding

This study was supported by the National Natural Science Foundation of China (Grant No. 32002178), the Key R&D Program of Shaanxi Province (Grant No. 2024NC-YBXM-096), the earmarked fund for CARS-35-PIG, the Undergraduate Training Program for Innovation and Entrepreneurship (Grant No. S202410712331), and the Overseas

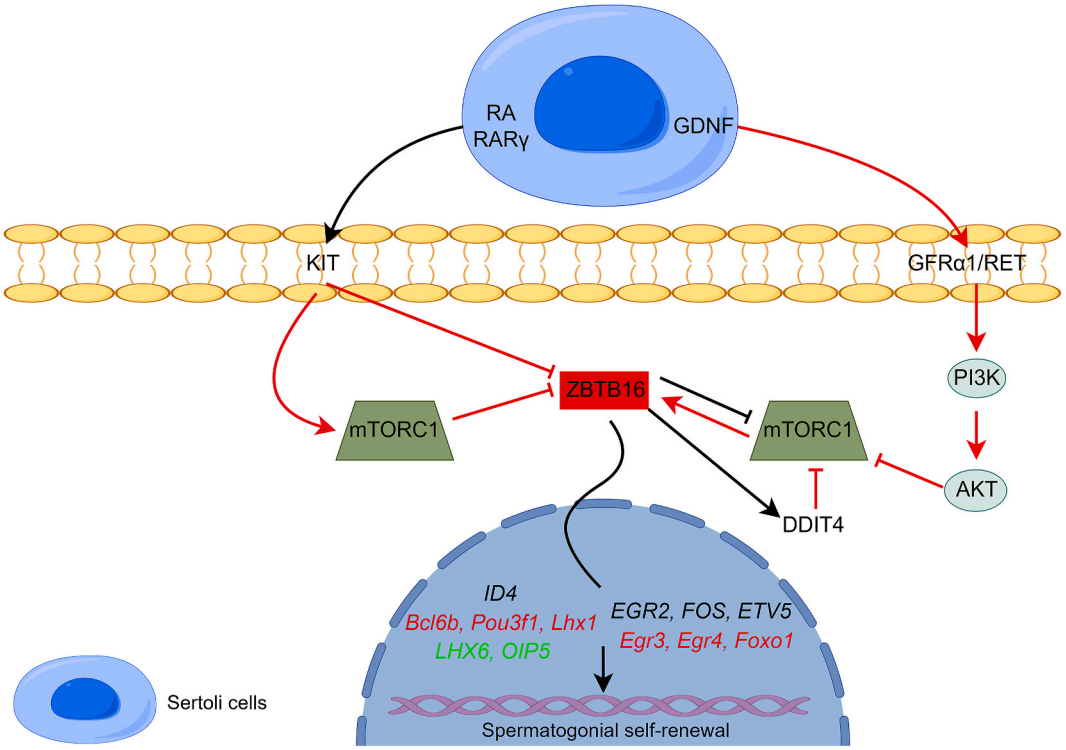


**Fig. 8.** A schematic overview of the regulatory repertoire of ZBTB16 in spermatogonia. The retinoic acid (RA) secreted by Sertoli cells suppresses ZBTB16 by upregulating KIT, or by indirectly upregulating mTORC1. GDNF, which could also be secreted by Sertoli cells, activates the PI3K/AKT signaling via its surface receptors GFRA1/RET on spermatogonia, further suppressing mTORC1 and upregulating ZBTB16. Besides, ZBTB16 can suppress mTORC1 via DDIT4. Subsequently, ZBTB16 promotes spermatogonial self-renewal through its target genes, such as *ID4*, *EGR2*, *FOS* and *ETV5*. Black, red and green colors refer to shared signaling and ZBTB16-target genes between porcine and murine spermatogonia, the reported signaling and ZBTB16-target genes in mice, and the pig-specific signaling and ZBTB16-target genes, respectively, based on this study and previous literature. (For interpretation of the references to color in this figure legend, the reader is referred to the Web version of this article.)

Students' Innovation and Entrepreneurship Individual Project of Ningxia (2021).

## Declaration of competing interest

The authors declare that there are no conflicts of interest.

## Appendix A. Supplementary data

Supplementary data to this article can be found online at https://doi.org/10.1016/j.theriogenology.2025.01.026.

## References

[1] Jan SZ, Hamer G, Repping S, de Rooij DG, van Pelt AMM, Vormer TL. Molecular control of rodent spermatogenesis. Biochim Biophys Acta (BBA) - Mol Basis Dis 2012;1822:1838–50.
[2] Zheng Y, Zhang L, Jin L, Zhang P, Li F, Guo M, et al. Unraveling three-dimensional chromatin structural dynamics during spermatogonial differentiation. J Biol Chem 2022;298:101559.
[3] Kubota H, Brinster RL. Spermatogonial stem cells. Biol Reprod 2018;99:52–74.
[4] Law NC, Oatley JM. Developmental underpinnings of spermatogonial stem cell establishment. Andrology 2020;8:852–61.
[5] Zheng Y, Gao Q, Li T, Liu R, Cheng Z, Guo M, et al. Sertoli cell and spermatogonial development in pigs. J Anim Sci Biotechnol 2022;13:45.
[6] Voigt AL, de Lima e Martins Lara N, Dobrinski I. Comparing the adult and pre-pubertal testis: metabolic transitions and the change in the spermatogonial stem cell metabolic microenvironment. Andrology 2023;11:1132–46.
[7] Voigt AL, Dardari R, Su L, Lara NLM, Sinha S, Jaffer A, et al. Metabolic transitions define spermatogonial stem cell maturation. Hum Reprod 2022;37:2095–112.
[8] Voigt AL, Kondro DA, Powell D, Valli-Pulaski H, Ungrin M, Stukenborg JB, et al. Unique metabolic phenotype and its transition during maturation of juvenile male germ cells. Faseb J 2021;35:e21513.
[9] Buaas FW, Kirsh AL, Sharma M, McLean DJ, Morris JL, Griswold MD, et al. Plzf is required in adult male germ cells for stem cell self-renewal. Nat Genet 2004;36:647–52.
[10] Costoya JA, Hobbs RM, Barna M, Cattoretti G, Manova K, Sukhwani M, et al. Essential role of Plzf in maintenance of spermatogonial stem cells. Nat Genet 2004;36:653–9.
[11] Costoya JA, Hobbs RM, Pandolfi PP. Cyclin-dependent kinase antagonizes promyelocytic leukemia zinc-finger through phosphorylation. Oncogene 2008;27:3789–96.
[12] Song W, Shi X, Xia Q, Yuan M, Liu J, Hao K, et al. PLZF suppresses differentiation of mouse spermatogonial progenitor cells via binding of differentiation associated genes. J Cell Physiol 2019;235:3033–42.
[13] Liu TM, Lee EH, Lim B, Shyh-Chang N. Concise review: balancing stem cell self-renewal and differentiation with PLZF. Stem Cell 2016;34:277–87.
[14] Reding SC, Stepnoski AL, Cloninger EW, Oatley JM. THY1 is a conserved marker of undifferentiated spermatogonia in the pre-pubertal bull testis. Reproduction 2010;139:893–903.
[15] Luo J, Megee S, Rathi R, Dobrinski I. Protein gene product 9.5 is a spermatogonia-specific marker in the pig testis: application to enrichment and culture of porcine spermatogonia. Mol Reprod Dev 2006;73:1531–40.
[16] Song W, Zhu H, Li M, Li N, Wu J, Mu H, et al. Promyelocytic leukaemia zinc finger maintains self-renewal of male germline stem cells (mGSCs) and its expression pattern in dairy goat testis. Cell Prolif 2013;46:457–68.
[17] Costa GM, Avelar GF, Rezende-Neto JV, Campos-Junior PH, Lacerda SM, Andrade BS, et al. Spermatogonial stem cell markers and niche in equids. PLoS One 2012;7:e44091.
[18] Borjigin U, Davey R, Hutton K, Herrid M. Expression of promyelocytic leukaemia zinc-finger in ovine testis and its application in evaluating the enrichment efficiency of differential plating. Reprod Fertil Dev 2010;22:733–42.
[19] Li T, Lv Y, Wu Z, Guo M, Liu R, Zeng W, et al. Systematic assessment of hexavalent chromium-induced damage to male fertility and the preventive role of melatonin: a longitudinal study from the translational point of view. Mol Hum Reprod 2023;29.
[20] Guo M, Li X, Li T, Liu R, Pang W, Luo J, et al. YTHDF2 promotes DNA damage repair by positively regulating the histone methyltransferase SETDB1 in spermatogoniadagger. Biol Reprod 2024;110:48–62.
[21] Zheng Y, Feng T, Zhang P, Lei P, Li F, Zeng W. Establishment of cell lines with porcine spermatogonial stem cell properties. J Anim Sci Biotechnol 2020;11:33.
[22] Goel S, Sugimoto M, Minami N, Yamada M, Kume S, Imai H. Identification, isolation, and in vitro culture of porcine Gonocytes1. Biol Reprod 2007;77:127–37.
[23] Park H-J, Lee R, Lee W-Y, Kim J-H, Do JT, Park C, et al. Stage-specific expression of Sal-like protein 4 in boar testicular germ cells. Theriogenology 2017;101:44–52.
[24] You X, Li T, Cui Y, Liu W, Cheng Z, Zeng W, et al. Retinoic acid-induced differentiation of porcine prospermatogonia in vitro. Theriogenology 2023;198:344–55.
[25] Hobbs RM, La HM, Makela JA, Kobayashi T, Noda T, Pandolfi PP. Distinct germline progenitor subsets defined through Tsc2-mTORC1 signaling. EMBO Rep 2015;16:467–80.
[26] Hobbs RM, Seandel M, Falciatori I, Rafii S, Pandolfi PP. Plzf regulates germline progenitor self-renewal by opposing mTORC1. Cell 2010;142:468–79.
[27] Du X, Yang D, Yu X, Wei Y, Chen W, Zhai Y, et al. PLZF protein forms a complex with protein TET1 to target TCF7L2 in undifferentiated spermatogonia. Theriogenology 2024;215:321–33.
[28] Szklarczyk D, Kirsch R, Koutrouli M, Nastou K, Mehryary F, Hachilif R, et al. The STRING database in 2023: protein-protein association networks and functional enrichment analyses for any sequenced genome of interest. Nucleic Acids Res 2023;51:D638–46.
[29] Lovelace DL, Gao Z, Mutoji K, Song YC, Ruan J, Hermann BP. The regulatory repertoire of PLZF and SALL4 in undifferentiated spermatogonia. Development 2016;143:1893–906.
[30] Filipponi D, Hobbs RM, Ottolenghi S, Rossi P, Jannini EA, Pandolfi PP, et al. Repression of kit expression by Plzf in germ cells. Mol Cell Biol 2007;27:6770–81.
[31] Oatley JM, Avarbock MR, Telaranta AI, Fearon DT, Brinster RL. Identifying genes important for spermatogonial stem cell self-renewal and survival. Proc Natl Acad Sci U S A 2006;103:9524–9.
[32] Chen SR, Liu YX. Regulation of spermatogonial stem cell self-renewal and spermatocyte meiosis by Sertoli cell signaling. Reproduction 2015;149:R159–67.
[33] Carnevalli LS, Trumpp A. Tuning mTORC1 activity for balanced self-renewal and differentiation. Dev Cell 2010;19:187–8.
[34] Hobbs Robin M, Fagoonee S, Papa A, Webster K, Altruda F, Nishinakamura R, et al. Functional antagonism between Sall4 and plzf defines germline progenitors. Cell Stem Cell 2012;10:284–98.
[35] Babatabar Darzi M, Nemati F, Azizi H, Dehpour Jouybari A. Immunohistochemistry and immunocytochemistry analysis of PLZF and VASA in mice testis during spermatogenesis. Zygote 2023;31:273–80.
[36] Oatley JM, Avarbock MR, Brinster RL. Glial cell line-derived neurotrophic factor regulation of genes essential for self-renewal of mouse spermatogonial stem cells is dependent on Src family kinase signaling. J Biol Chem 2007;282:25842–51.
[37] Lee J, Kanatsu-Shinohara M, Inoue K, Ogonuki N, Miki H, Toyokuni S, et al. Akt mediates self-renewal division of mouse spermatogonial stem cells. Development 2007;134:1853–9.